

Superconductive Supercooling and Superheating of Small Cadmium Spheres: Size Effects*

Francisco de la Cruz, M. David Maloney, and Manuel Cardona
Department of Physics, Brown University, Providence, Rhode Island 02912
 (Received 7 December 1970)

Supercooling and superheating have been observed for samples composed of small cadmium spheres of uniform well-defined sizes. The data obtained for large sphere diameters are independent of size and represent, by all indications, ideal bulk properties. The supercooling data for such spheres have been used to obtain the Ginsburg-Landau parameter κ and, in conjunction with BCS expressions, the penetration depth λ and the coherence length ξ_0 . The temperature dependence of the supercooling field H_{sc} shows an anomaly for $t \sim 0.8$, very similar to that previously reported for Al and Zn. The superheating field of these "bulk" spheres shows strong effects of the nonlocal electrodynamics below T_c . Spheres of diameters equal to or smaller than 10μ show strong size effects in the supercooling and superheating fields, especially near T_c . The results are examined in the light of existing theories of critical fields for small spheres. A systematic decrease of the critical temperature with sphere size has also been observed. It seems related to a decrease in the gap anisotropy, produced by boundary scattering. These results are analyzed in terms of the theory of Markowitz and Kadanoff.

I. INTRODUCTION

The Ginsburg-Landau parameter κ can be determined from either the supercooling or superheating field of bulk superconductors when the metastable states occur to their ideal limit.¹⁻⁷ The theoretical relationship between the bulk supercooling H_{sc} and superheating H_{sh} fields and the thermodynamic critical field H_{cb} , was derived by Ginsburg⁸ by solving the appropriate Ginsburg-Landau equations. He found for $1-t \ll 1$

$$H_{sc} = H_{c2} = \sqrt{2} \kappa H_{cb}, \quad (1)$$

$$H_{sh} = 2^{-1/4} \kappa^{-1/2} H_{cb}. \quad (2)$$

Equations (1) and (2) should be valid very near T_c . Saint-James and de Gennes⁹ pointed out that the nucleation of the superconductivity in decreasing fields does not occur in the bulk [Eq. (1)] but at portions of the surface parallel to the magnetic field. In order to take into account this fact, the Ginsburg-Landau equations must be solved with the appropriate boundary conditions: It is found that the supercooling field given by Eq. (1) must be multiplied by 1.695. The new supercooling field, usually referred to as H_{c3} , thus becomes

$$H_{sc} = H_{c3} = 1.695 H_{c2} = 2.4 \kappa H_{cb}. \quad (3)$$

Equation (3) is valid for $1-t \ll 1$. At lower temperature we can use it to define a phenomenological parameter κ_{sc}

$$H_{sc}(t) = 2.4 \kappa_{sc}(t) H_{cb}. \quad (4)$$

The $\kappa_{sc}(t)$ is not very strongly temperature dependent.

Although Eq. (3) is valid for $1-t \ll 1$ (typically $1-t < 0.1$), the requirements of validity of Eq. (2)

are considerably more stringent for pure type-I materials. Equation (2) was derived under the assumption of local electrodynamics which only hold for $\lambda(t) > \xi_0$, i. e., for $1-t < \kappa^2$. Thus the region of validity of Eq. (2) is extremely small for materials with $\kappa \sim 0.01$, such as Al, Zn and, as we shall see, Cd. It is also conventional to use Eq. (2) to define a temperature-dependent phenomenological parameter $\kappa_{sh}(t)$. For $t=1$ we must have $\kappa_{sh}(1) = \kappa_{sc}(1) = \kappa$. If the nonlocal nature of the electrodynamics is taken into account one finds, in the temperature range $1 \gg 1-t \gg \kappa^2$,¹⁰

$$H_{sh} = C(1-t)^{-1/12} \kappa^{-1/3} H_{cb}, \quad (5)$$

with $C \sim 1.36$.

No attempts have been made to remove the restriction $1-t \ll 1$ from the superheating-field calculation. Attempts have been made, however, to calculate the supercooling field at all temperatures, this calculation being easier than for H_{sh} because it deals only with linearized equations. The temperature dependence of κ_{sc} [Eq. (4)] can be decomposed into two parts, that arising from the temperature dependence of H_{c2}/H_{cb} ,¹¹⁻¹³ and that from the temperature dependence of H_{c3}/H_{c2} .^{14,15}

The theoretical expressions given above for H_{sc} and H_{sh} apply to "bulk" samples of dimensions large compared with the temperature-dependent coherence length $\xi(t)$. When any of the sample dimensions becomes of the order of ξ , size effects appear and the expressions for H_{sc} and H_{sh} must be modified. Since $\xi(t)$ diverges like $(1-t)^{-1/2}$ near $t=1$, any sample of finite size will show size effects sufficiently close to T_c . For sufficiently small samples, the magnetic transition changes from first order to second order^{9,16,17} and metastable states disappear. For spherical samples this happens when the radius

becomes smaller than the critical radius $R_c = 2.29\lambda$,⁸ where λ is the penetration depth. As we shall see the radius of the Cd spheres used in this work ($R > 5000 \text{ \AA}$) is always larger than $\lambda(t)$, even near T_c , and hence metastable states are expected to occur in all samples measured. Nevertheless, Eqs. (2) and (4) have to be modified so as to take into account the fact that $\xi(t)$ may be of the order of R . For spherical samples and in the limit $\xi(t) \gg R$ Ginzburg⁸ found that Eqs. (2) and (4) must be replaced by

$$H_{sc} = 2\sqrt{5} H_{cb} \lambda / R, \quad (6)$$

$$H_{sh} = 0.407 H_{cb} (\lambda/R)^{1/2}. \quad (7)$$

The derivation of Eq. (6) assumes local electrodynamics. This equation must be modified for clean type-I materials since the vector potential A varies rapidly over a Pippard coherence length, defined by $1/\xi = 1/\xi_0 + 1/l$, where l is the electron mean free path and ξ_0 is the coherence length for the pure material. If this coherence length is larger than the smallest dimension of the sample, nonlocality effects will appear even at $T = T_c$. Assuming $\xi(t) \gg R$ in order to obtain an order parameter constant throughout the sample, Tinkham and de Gennes¹⁸ found

$$H_{sc}(t)/H_{cb}(0) = 4.85\lambda_L \xi_0^{1/2} / R^{3/2} f(t), \quad (8)$$

where λ_L is the London penetration depth at $T = 0$ and $f(t)$ a function plotted in Ref. 18. The function $f(t)$ can be approximated well by the temperature dependence obtained from the two-fluid model¹⁸

$$f(t) = (1 - t^2)^{1/2} / (1 + t^2)^{1/2}.$$

No calculations are available for the size effect on the superheating field in the nonlocal case.

From the experimental point of view, the determination of κ_{sc} and H_{sh} and the observation of the size effects discussed above require the preparation of samples sufficiently perfect to yield the theoretical metastability limits of H_{sc} and H_{sh} . Defects of almost any kind tend to reduce the range of fields for which the metastable states are possible. The most successful technique for the preparation of such samples was developed by Feder *et al.*³ The sample consists of a collection of well-separated small spheres, some of which at least will exhibit ideal behavior. H_{sc} and H_{sh} are thus observed as the fields at which the traces of either normal or superconducting behavior disappear. The superheating measurement (and not the supercooling) requires corrections of the effect of demagnetizing fields. The application of these corrections is made easier by using spheres. This technique has been also used by other authors.²⁻⁷ The measurement of both

supercooling and superheating provides a simple test of the ideal nature of these phenomena in the particular sample under study: κ_{sc} and κ_{sh} should extrapolate to the same value for $T = T_c$. This constitutes a test of ideal behavior together with the reproducibility of the results obtained for samples prepared by different techniques. We point out that ideal behavior near T_c does not guarantee ideal behavior at lower temperatures. Small defects which limit ideal behavior at low temperatures may become ineffective near T_c since the coherence length increases as $(1 - t)^{-1/2}$. Such defects may produce a temperature variation of κ_{sc} and κ_{sh} larger than the ideal one.⁴ A peculiar temperature dependence of κ_{sc} was found for two extremely nonlocal superconductors, Al and Zn.² No temperature dependence was detected from T_c to a reduced temperature $t \sim 0.85$; then a very rapid stepwise increase took place until $t \sim 0.70$. From $t = 0.70$ until the lowest temperatures reached κ_{sc} is again almost temperature independent. As pointed out² technical difficulties in the preparation of the sample made it impossible to obtain homogeneity in the size of the spheres. The size inhomogeneity might have been invoked to explain the anomalous behavior observed. The argument would go as follows: Owing to the definition of H_{sc} used in Ref. 2 the spheres that supercool most are the ones that determine H_{sc} . At temperatures close to T_c size effects could increase the supercooling field for the smaller spheres and the largest ones would determine H_{sc} ; at lower temperatures however, nonideality of the largest spheres would make H_{sc} be determined by the smaller ones.

The Al and Zn samples just discussed were prepared by spraying the molten metal into liquid nitrogen. In order to ascertain the ideality of the strong temperature dependence of κ_{sc} just described, we prepared samples composed of spheres of uniform well-defined sizes. The material chosen for our studies was Cd. Its superconducting properties are rather similar to those of Al and Zn but its lower melting point permits the preparation of spheres by ultrasonic dispersion into hot oil. The sonoration process was followed by a suitable decantation so as to separate spheres of approximately the same size.

We have been able to show that the peculiar temperature dependence found in Al and Zn is also obtained for Cd and that neither the spread in sphere size nor any nonideal properties of the sample are the causes of such behavior. The Cd samples so prepared have also enabled us to study size effects on H_{sc} , H_{sh} , and on the critical temperature at zero field. All these effects seem to require for theoretical interpretation a value of ξ_0 much smaller than that obtained from H_{cb} and the κ found for the largest samples.

II. SAMPLE PREPARATION

The samples were prepared by ultrasonic dispersion (sonorizing) of the molten metal into Dow Corning 210-H fluid. The boiling point of this fluid is about 350 °C and the melting point of Cd is 320 °C.

The metal (Johnson-Matthey 99.999% Cd) was placed into a beaker containing the oil and heated until the metal melted. The tip of an ultrasonic cutter was placed in the proximity of the metal, thus producing the desired dispersion. The average size of the particles depends on the ultrasonic power and on the duration of the sonorizing process. Immediately after sonorizing the metal, the oil was cooled and the particles were cleaned using different solvents. In this way a shiny particle surface is obtained; the particles are spherical with diameters ranging from 1 to about 50 μ . To obtain good separation by size the spheres were decanted in different liquids (acetone, toluene, trichlorethylene, and alcohol) for different lengths of time, and those reaching certain levels in the liquid were collected. It was thus possible to obtain collections of spheres of nearly the same size with standard deviations, usually less than 10%. The size of the spheres (between 50 and 4 μ) was determined by microscopic examination and comparison with a graduated scale. The sizes of the 1- μ spheres were determined with an electron microscope. To avoid distortion of the magnetic field due to proximity of the spheres the sample powder was diluted using a solution of alcohol saturated with sodium oleate; only one-tenth of the total volume was occupied by the spheres.

III. TECHNIQUE OF MEASUREMENT

The sample was placed inside a pair of coils and the field transitions were determined by the variation of the mutual inductance detected with a bridge.¹⁹ The 1000-Hz ac magnetic field produced by the primary was perpendicular to the applied dc field, and smaller than 50 mOe. More details about the experimental arrangement will be published elsewhere.² To obtain the desired range of temperature ($T_c = 0.52$ °K), a conventional He³ cryostat was used.² The sample was immersed inside the cryogenic liquid to ensure good thermal contact. Different temperatures were obtained by varying the pressure of the He³. Temperature regulation was obtained by controlling the pumping speed of the system. The temperature was determined with two carbon resistor thermometers used in different temperature ranges so as to optimize the sensitivity. Their resistance was measured with an ac bridge operating at 33 Hz. Owing to the low vapor pressure of He³ in the desired temperature range, the thermometers were calibrated by measuring the critical field of an Al cylinder, 3 mm

in diameter and 12 mm long. The same mutual inductance used for the Cd samples was used to detect the transition field of the Al cylinder. The cylinder and mutual inductance were immersed in the liquid He³. The carbon resistors were outside the bath in the vacuum jacket thermally connected to the bath by means of a copper rod of 4-mm diam and 40-mm length screwed to the bottom of the He³ container. The thermometers were placed inside holes of appropriate dimensions in the copper rod with Apeizon-N grease to improve the thermal contact. Between 1.2 and 0.5 °K the vapor pressure of the He³ was used as an absolute thermometer; readings of both the carbon resistors and the vapor pressure were taken when performing measurements. The transition width observed for the cylinder at zero field was ~ 3 m°K. The values obtained for the critical temperature and critical fields with the vapor pressure thermometer agree to better than 1% with the values reported by Harris and Mapother.²⁰ We have made several calibrations using the same method, and the critical field value for the Al cylinder always agreed to within $\pm 1\%$. The critical field of Al measured by Harris and Mapother²⁰ was used to calibrate the carbon resistors between 0.5 and 0.3 °K. The accuracy in the temperature determination using this method is about $\pm 1\%$.

The experimental set up allows us to change samples without removing the resistors from the copper rod; no new wire solderings are performed between experiments. In this manner the thermometer calibration does not change within the experimental accuracy from one set of measurements to another.

Owing to the very small field at which supercooling occurs, it was necessary to compensate for the earth's magnetic field. Using a pair of Helmholtz coils the vertical component of the earth's magnetic field was reduced below 10 mOe. The effect of the horizontal component was corrected by measuring the transitions for opposite directions with the field parallel to the horizontal component. The field was measured with a Hall probe magnetometer (RFL Model 1890, Radio Frequency Labs., Inc., Boonton, N. J.). All magnetic materials were carefully avoided near the cryostat and all the superconducting soldering was placed as far as possible from the sample. During the first measurements a remanent field of the order of 0.1 Oe was discovered, despite all precautions. This field suppressed the supercooling transitions at temperatures close to T_c . The remanent field was produced by the carbon resistors, probably due to currents induced in the internal copper leads of the thermometers lined with a superconducting metal. The minimum remanent field, for a given distance between the thermometer and the sample, was found when the applied field was perpendicular

to the axis of the resistor. By increasing the distance between the sample and the thermometers we are able to reduce the remanent field below 10 mOe. This situation obtained when the thermometers were 3 cm from the sample and the magnetic field was applied perpendicular to the thermometer axis.

IV. RESULTS

To determine the thermodynamic critical field of our cadmium, a cylinder 2 mm in diameter and 15 mm long was measured. This cylinder was prepared from a $\frac{1}{4}$ -in. rod of the same material used to prepare the spheres. It was annealed in vacuum at 150 °C; after annealing the surface was chemically polished using an aqueous solution of 75% HNO₃. For increasing fields it was possible to stabilize the signal at any value between the maximum and the minimum signal at all temperatures. This indicates that no superheating was present. However, a considerable amount of supercooling was detected in decreasing fields. To obtain this supercooling the magnetic field must be increased to a certain minimum value (quenching field) above the critical field at this temperature. This effect has been observed in other materials²¹ and seems related to the existence of small regions inside the metal that remain superconducting at fields higher than the critical field. Figure 1 shows the results for the critical field and the quenching and supercooling fields of the cylinder. It can be seen that the extrapolation of the quenching field to zero

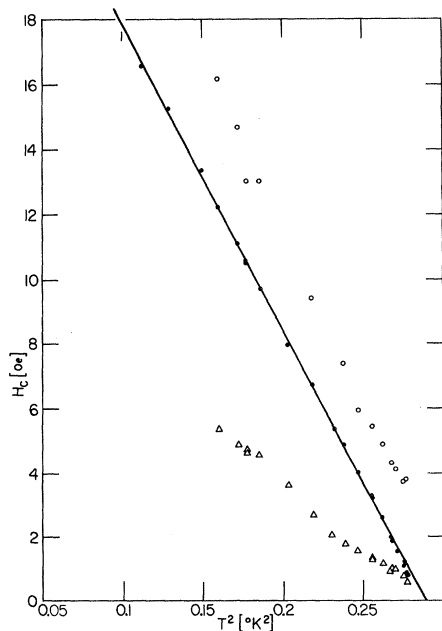


FIG. 1. Magnetic transitions of a cadmium cylinder. O, quenching field; ●, thermodynamic critical field; Δ, supercooling field.

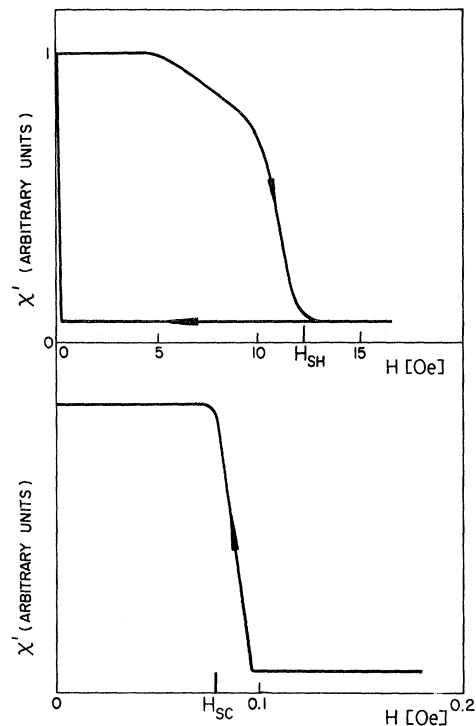


FIG. 2. Typical hysteresis loop (in the case for 50- μ Cd spheres at $t=0.95$). The lower curve shows the supercooling transition with an expanded horizontal scale.

field gives a higher critical temperature than the one defined from the thermodynamic critical field. The critical temperature T_c defined from the extrapolation of the thermodynamic critical field is $T_c = 0.536 \pm 0.002$ °K. The experimental data for H_c can be fitted to an expression of the form $H = H_0(1 - t^2)$. The value obtained from this fitting for the critical field at zero temperature is $H_0 = 27.3 \pm 0.1$ Oe.

Samples composed of spheres of 1-, 4-, 10-, 20-, and 50- μ diam were measured. Large supercooling and superheating was observed in all of them. A typical transition for the 50- μ samples is shown in Fig. 2. Different x scales were used in the recorder in order to obtain an accurate definition of H_{sc} and H_{sh} . The transitions observed for Cd are much sharper than the ones obtained previously for Al and Zn,² due probably to a better quality of the the sample (the Al and Zn samples, of higher melting point, were prepared by spraying). Figure 3 shows the supercooling fields as a function of the reduced temperature for several sphere sizes. The results for the 20- μ sample coincide with those for the 50- μ one and are not shown in order to avoid confusion. For the same reason, a smooth line is drawn instead of the points for the 10- μ sample. Figure 4 shows the observed superheating fields as a function of reduced temperature. The results

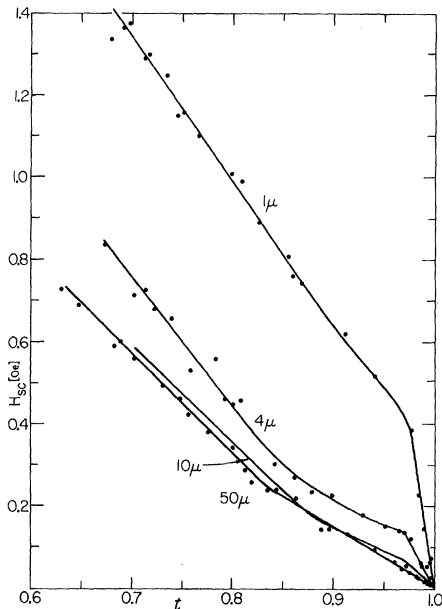


FIG. 3. Supercooling field measured as a function of reduced temperature for spheres of several sizes.

for the 50-, 20-, and 10- μ samples are the same within the experimental error. The points plotted in Fig. 4 correspond to the 50- μ sample; only smooth lines are shown for the 1- and 4- μ samples. The smaller samples (4 and 1 μ) clearly exhibit size effects. The supercooling and superheating fields seem to change in a monotonic way with thickness, thus indicating that the observed change is a real size effect. No size effect seems to be present in the 50- μ samples and by all indications the observed transition corresponds to ideal bulk superheating.

The transition temperature for each sample was determined by extrapolation of the supercooling and superheating data to zero field. The temperatures obtained from both extrapolations coincide to $\pm 10^{-3}$ $^{\circ}$ K. The transition width at zero field was about 5×10^{-3} $^{\circ}$ K.

A systematic and well-determined decrease of the critical temperature with the size of the spheres was observed. The critical temperature for different samples has been plotted in Fig. 5; an extrapolation to infinite size gives a critical temperature of $(0.532 \pm 0.002)^{\circ}$ K. This value is only slightly lower than the one obtained for our cylinder (0.536 $^{\circ}$ K).

We have used expressions (2) and (4) to define and calculate the effective values of κ_{sc} and κ_{sh} from the experimental data. The results are shown in Figs. 6 and 7; the bars in the figure indicate the estimated experimental error in different temperature regions. To account for the shift in critical temperature with sample size a reduced temperature

representation is used. The critical thermodynamic field H_{cb} used for the evaluation of κ_{sc} and κ_{sh} is the one obtained from the bulk cylinder, but with a critical temperature equal to that of the spheres under consideration. It can be seen in Figs. 3, 4, 6, and 7 that the supercooling fields for 10-, 4-, and 1- μ samples show size effects in all the temperature range. However, it is interesting to note that, for the same samples and temperature range, size effects in the superheating field disappear for temperatures lower than $t = 0.82$. Several samples of spheres of a given size were measured; the results for each size were always the same, thus suggesting that ideal size effects were being observed.

V. DISCUSSION

A. Bulk Sample

The results shown in Figs. 3 and 4 indicate very strongly that the transition fields of the 50- μ samples are the size-independent bulk fields. A comparison of these results to those of Al and Zn² shows that the temperature dependence of the bulk κ_{sc} is quite similar for all those materials. In Fig. 8 we have plotted for comparison κ_{sc} of Zn and Al² together with the corresponding parameter obtained here for the 50- μ Cd spheres. We have also plotted, in the same figure, several possible theoretical temperature dependences for κ_{sc} . The open circles represent the temperature dependence predicted by Gorkov¹¹; the dots correspond to the variation with temperature predicted by Gorkov, corrected for the temperature dependence of H_{c3}/H_{c2} ,

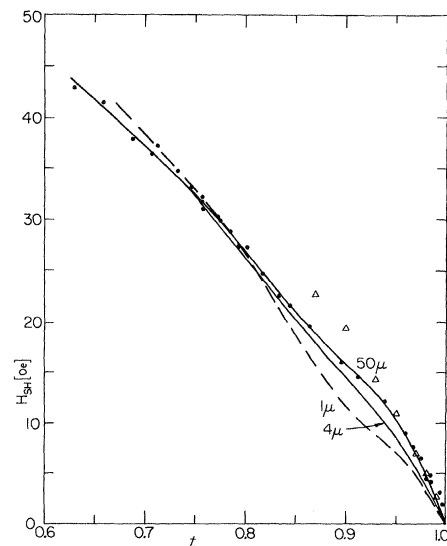


FIG. 4. Superheating field measured as a function of reduced temperature for Cd spheres of several sizes. The triangles are points calculated with Eq. (5) for $C = 1$.

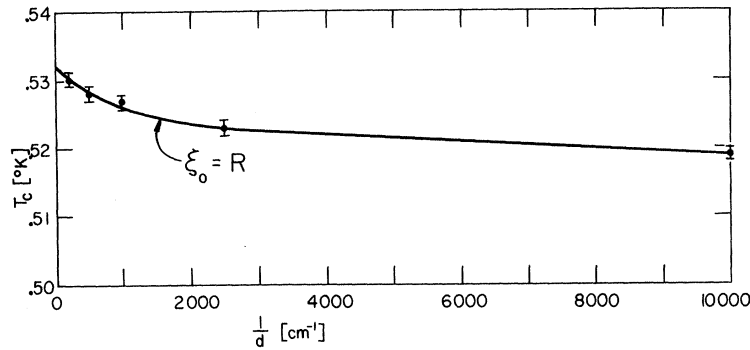


FIG. 5. Critical temperature as a function of the inverse diameter of the Cd spheres.

for the case of diffuse scattering.¹⁴ The crosses represent the phenomenological two-fluid model.²² Although the total experimental variation of κ_{sc} shown in Fig. 8 is not much larger than the one using the temperature dependence of $\kappa(t)$ ¹¹ and H_{c3}/H_{c2} ,¹⁴ no detailed agreement is found between theory and experiment.

Our measurements for Cd give $\kappa_{sc}(t=1) = 0.012$, in good agreement with the extrapolation of κ_{sh} to $t=1$. A fair agreement between expression (5) and the results for H_{sh} was found near T_c . In Fig. 4 the triangles are points obtained from expression (5) with $\kappa = 0.012$ and $C = 1$. In order to make κ in expression (5) coincide with κ_{sc} at $t=1$, it was necessary to choose for C a lower value than the theoretical 1.36. While the significance of this fact is not known, we point out that values of C also close to 1 are necessary to fit similar data for Sn, In,¹⁰ Al, and Zn.²

From the value of $\kappa(t=1)$ and the slope of the critical field at T_c it is possible to calculate the London penetration depth $\lambda_L(0)$ at $T=0$. Neglecting energy-gap and band-structure anisotropies²³ the BCS theory yields the expression²²:

$$\kappa^2 = \frac{2e^2}{\hbar^2 c^2} \left| \frac{dH_0}{dT} \right|_{T=T_c}^2 \lambda_L^4(0) T_c^2. \quad (9)$$

Using our experimental values for $H_c(T)$, T_c , and $\kappa(t=1)$, Eq. (9) yields $\lambda_L(0) = 315 \text{ \AA}$. Similarly, from the relation $\kappa = 0.96 \lambda_L(0)/\xi_0$, we obtain for Cd $\xi_0 = 25000 \text{ \AA}$, where we emphasize again the fact that anisotropy effects have been neglected.²³

B. Size Effects

As was said before, no size effects were detected in the 50- and 20- μ samples. The first sample that shows a size effect is that composed of 10- μ -diam spheres. Baratoff and Bergeron²⁴ have found an expression for H_{c3} for a sphere of radius R as a function of $R/\xi(T)$, valid for $(1-t) \ll 1$ and $R \gg \xi(t)$:

$$\frac{H_{c3}(R)}{H_{c3}(\infty)} = 1 - 0.65 \left(\frac{\xi(t)}{R} \right)^{2/3} + 2.19 \frac{\xi(t)}{R} + O \left(\frac{\xi(t)}{R} \right)^{4/3} + \dots \quad (10)$$

This result can be understood qualitatively in the following way. When the radius of curvature of

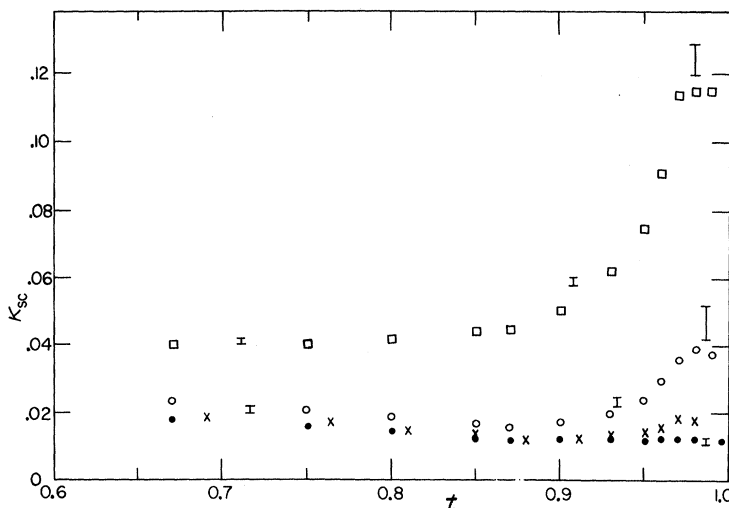


FIG. 6. The $\kappa_{sc}(t)$ for Cd spheres of several diameters, \square , $d = 1 \mu$; \circ , $d = 4 \mu$; \times , $d = 10 \mu$; \bullet , $d = 50 \mu$.

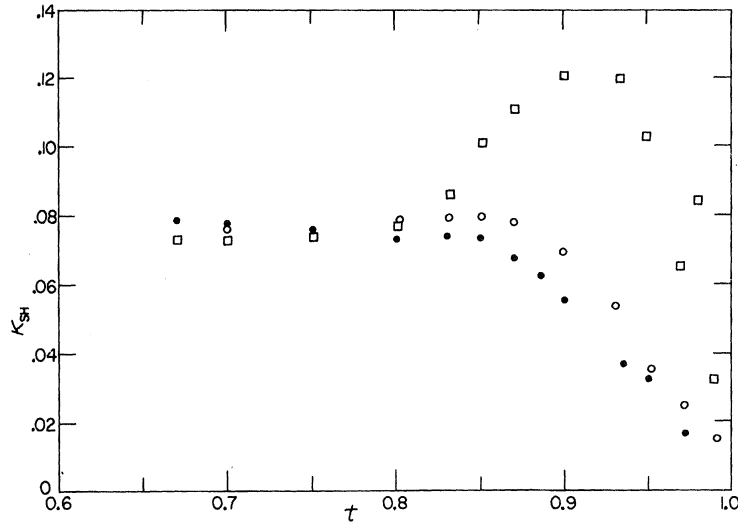


FIG. 7. The $\kappa_{sh}(t)$ for Cd spheres of several diameters, \square , $d=1\mu$; \circ , $d=4\mu$; \bullet , $d=50\mu$.

the sample is much larger than ξ , the nucleation occurs in that portion of surface around the equatorial plane that can be assumed flat and parallel to the field. When the coherence length becomes of the order of R , the nucleation field should decrease [$(\xi/R)^{2/3}$ term in Eq. (10)] because the nucleation does not strictly take place in a surface parallel to the field. At the same time the usual size effect, discussed in the Introduction, tends to increase the transition field [ξ/R term in Eq. (10)]. The relative importance of each of these competing effects depends on the value of ξ/R . Using Eq. (10) with the value obtained for the coherence length of Cd ($\xi_0 = 2.5 \mu$) and the appropriate temperature dependence [$(1-t)^{-1/2}$], it can be seen that an appreciable size effect is expected even for the 50- μ spheres. This effect is not observed experimentally; thus either the coherence length is smaller than our estimate or Eq. (10) overestimates the size effects. If Eq. (10) is assumed to be correct, one must have $\xi(t=0) < 0.2 \mu$ in order to eliminate size effects for the 50- μ spheres. Even in this case a size effect would be expected for the 20- μ spheres. It is very unlikely that the neglected gap and band-structure anisotropy²⁵ will change the estimated $\xi(t=0)$ to values below 0.2 μ . The experimental

results thus suggest that Eq. (10) grossly overestimates the size effects in large spheres.

Let us consider now the 1- μ sample. Here the coherence length is larger than the size of the spheres throughout the whole temperature range. Consequently, we can expect Eq. (8) to apply. Figure 9 shows a plot of the ratio H_{sc}/H_{cb} as a function of $(1-t^4)^{-1/2}$ for the 1- μ sample; it is obvious that the expected temperature dependence is not found. In view of the discrepancy between observed and predicted temperature dependence of H_{sc} for thicker samples, the present discrepancy for thinner samples is not too surprising. The anomalous kink observed for the 50- μ (bulk) spheres in Fig. 3 at $t=0.84$ is also present for the 10- μ and 4- μ spheres. The effect of this anomalous temperature dependence on the supercooling field of the small spheres would be diminished if we plotted the ratio of this field to the corresponding field of the 50- μ spheres. Using expressions (4) and (8) we find

$$\frac{H_{sc}(d=1)}{H_{sc}(d=50)} = \frac{\lambda_{eff}}{1.695R\sqrt{2}\kappa(t)} \frac{f(t)}{(1-t^2)},$$

where $\lambda_{eff} = 4.85\lambda_L\xi_0^{1/2}/R^{1/2}$ and $R = 5 \times 10^{-5}$ cm is the radius of the small spheres. Using the two-fluid model to approximate¹⁸ $f(t)$ and the tempera-

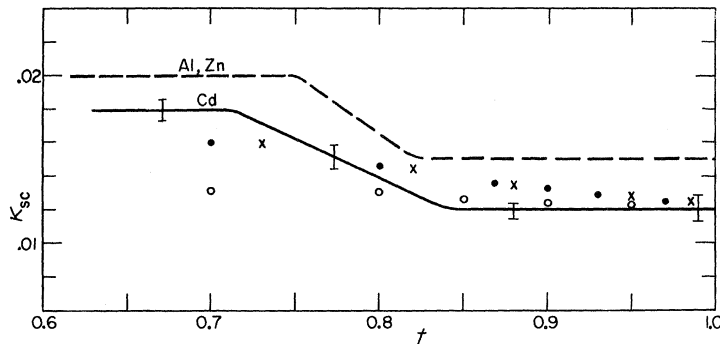


FIG. 8. Experimental results for κ_{sc} for the 50- μ Cd spheres and those for Al and Zn reported in Ref. 2. Expected values for $\kappa_{sc}(t)$ using different possible theoretical temperature dependences, as indicated in the text.

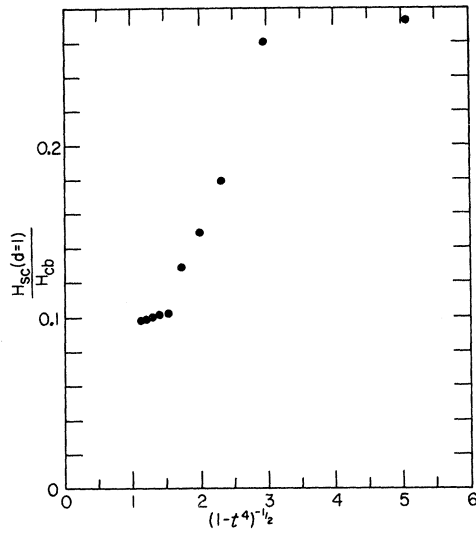


FIG. 9. Ratio of the supercooling field for sample of 1- μ diam to the thermodynamic critical field as a function of $(1-t^4)^{-1/2}$.

ture dependence for $\kappa(t)$ given by the same model²² we have

$$\frac{H_{sc}(d=1)}{H_{sc}(d=50)} = \frac{\lambda_{eff}}{2\sqrt{2} \cdot 1.695 R \kappa(t=1)} \left(\frac{1+t^2}{1-t^2} \right)^{1/2}. \quad (11)$$

Figure 10 shows a plot of the experimental ratio $H_{sc}(d=1)/H_{sc}(d=50)$ as a function of $(1+t^2)^{1/2}/(1-t^2)^{1/2}$. Except for the points very close to T_c , the temperature dependence of this ratio is very well described by Eq. (11). The slope of the straight line in Fig. 10 is given by $\alpha \sim (\xi_0/R)^{3/2}$. If we use the value $R = 5 \times 10^{-5}$ cm for the small spheres and the experimental value of α , we get $\xi_0 = 0.60 \mu$. This value is smaller by a factor of 4 than the value obtained from the supercooling and superheating fields of the bulk spheres. Here again, the size effect predicted theoretically is much larger than the one observed.

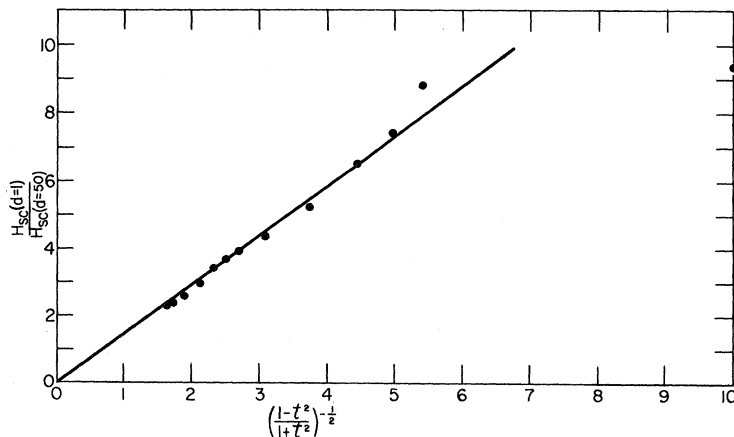


FIG. 10. Ratio of the supercooling field of the sample of 1 μ to that of the 50- μ sample as a function of $(1+t^2)^{1/2}/(1-t^2)^{1/2}$.

The decrease in the critical temperature with decreasing sphere size, shown in Fig. 5, can also be attributed to a size effect. It is well known²⁵⁻²⁷ that a decrease in the critical temperature of a pure superconductor can be produced by doping it with nonmagnetic impurities. Markowitz and Kadanoff²⁵ have attributed this effect to the decrease in the gap anisotropy associated with the decrease in the mean free path produced by the doping. If no other effect is produced by the doping (e.g., valence effects), this decrease of critical temperature continues until the electronic mean free path is of the order of the coherence length.²⁵ Markowitz and Kadanoff²⁵ assume an anisotropic pairing interaction of the form

$$V_{pp'} = [1 + a(\vec{\Omega})] V[1 + a(\vec{\Omega}')],$$

where $\vec{\Omega}$ is a unit vector along the direction of the quasiparticle momentum \vec{p} , and $a(\vec{\Omega})$ is the anisotropy function defined so as to have zero average. Under these conditions, the decrease in T_c due to the impurities is

$$\Delta T_c = K^1 \chi - 0.36 \langle a^2 \rangle T_c \chi + 7.8 \times 10^{-2} \langle a^2 \rangle \chi T_c \ln \chi, \quad (12)$$

where the doping parameter χ is given by

$$\chi = \frac{\hbar/\tau_a}{kT_c} = \frac{\xi_0/\tau_a}{A\bar{v}_F}. \quad (13)$$

In Eq. (13), τ_a is a scattering time appropriate to the removal of gap anisotropy²⁵ by the impurity and \bar{v}_F is an average of the Fermi velocity. The BCS theory gives for the constant A the value 0.18.

This equation is a good approximation to the numerical calculation²⁵ in the range $1 < \chi < 100$. The first term in the right-hand side of Eq. (12) represents effects of the doping other than the removal of gap anisotropy. Its magnitude depends on the type of dopant and, in particular, its valence.

The presence of boundaries in small samples pro-

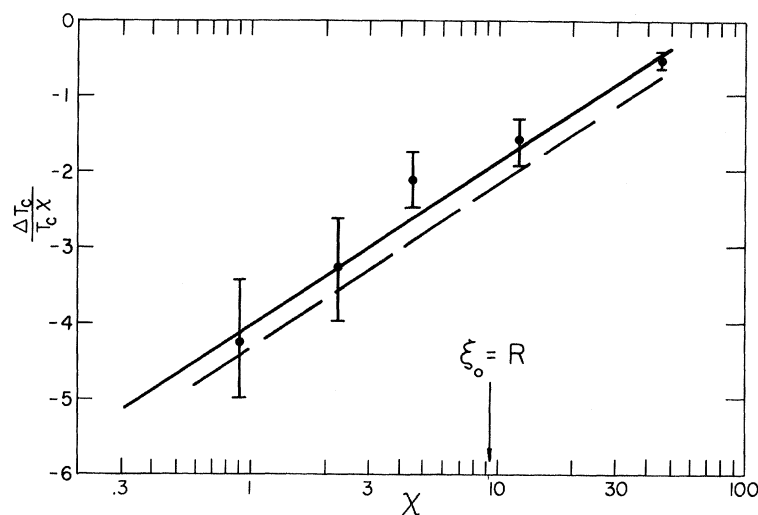


FIG. 11. $\Delta T_c/T_c \chi$ as a function of $\ln \chi$. ●, experimental points; the dashed line was obtained from expression (10) as explained in the text.

duces a decrease in the mean free path which should also effect a decrease in the anisotropy of the gap. Such effect has been observed^{28,29} in In and Ga and shown to be in qualitative agreement with Eq. (12). On the basis of this argument, a decrease in the particle size should result in a decrease in the critical temperature describable by Eq. (12) with $K^i = 0$. For a quantitative discussion of the results of Fig. 5, one must establish the relationship between sphere size and effective electronic mean free path. In view of the uncertainties in the scattering process at the surface of the sphere, we simply assume that the mean free path is close to the radius of the sphere R . Under these assumptions Eq. (13) becomes

$$\chi = \xi_0 / AR. \quad (14)$$

Using³⁰ $\bar{v}_F = 1.63 \times 10^8$ cm sec⁻¹, $\xi_0 = 2.5 \times 10^{-4}$ cm, the value determined here, and $T_c = 0.536$ °K, we find from Eq. (13) a value of the dimensionless parameter $A = 0.11$, somewhat smaller than that predicted by the BCS theory ($A = 0.18$) in the absence of anisotropy corrections.²³ We shall use $A = 0.11$ in our discussion. The size dependence of T_c should become weaker for $l \sim R < \xi_0 = 2.5 \mu$. The results of Fig. 5 agree with this estimate. In order to perform a more quantitative analysis we plot in Fig. 11, $\Delta T_c/T_c \chi$ as a function of $\ln \chi$: According to Eq. (12) we should obtain a straight line whose slope should yield the anisotropy parameter $\langle a^2 \rangle$. The experimental points fall, within the experimental error, on a straight line; from the slope of the line we find $\langle a^2 \rangle = 0.012$. From the intercept of this line the parameter K^i of Eq. (12) can be obtained. As mentioned earlier for boundary scattering we expect this parameter to be close to zero. The dashed line in Fig. 11 corresponds to $K^i = 0$ and lends support to this contention.

The anisotropy parameter $\langle a^2 \rangle = 0.012$ is similar

to that of Al,²⁵ a somewhat surprising fact since Cd is considerably more anisotropic than Al. Ducla-Soares and Cheeke³¹ recently reported $\langle a^2 \rangle = 0.05$ for Cd and $\langle a^2 \rangle = 0.02$ for Zn, also a highly anisotropic material. The accuracy of their determination is not known. It is worthwhile to note that a higher slope is obtained in Fig. 11 if χ is multiplied by a factor smaller than 1, i. e., if either ξ_0 is decreased or the mean free path increased. When this is done K^i becomes no longer negligible. In order to obtain $\langle a^2 \rangle \approx 0.04$, χ must be divided by 3 and K^i becomes equal to -5.2×10^{-3} (°K). We cannot offer any physical interpretation for this possible nonvanishing value of K^i . Here again, as in the case of the size effects on the supercooling and superheating fields, in order to obtain agreement with independent values of $\langle a^2 \rangle$, we are forced to accept very small values of ξ_0/l . Either the required coherence length ξ_0 disagrees with our determination for bulk samples or the mean free path is considerably larger than the sphere radius R .

VI. CONCLUSIONS

The anomalous behavior of κ_{sc} found² for Al and Zn is also present in Cd and, by all indications, seems to be a property of bulk ideal samples of these materials. For small Cd spheres, size effects appear but the sphere sizes at which these effects become noticeable are considerably smaller than one would expect on the basis of the ξ_0 determined for the bulk samples. In order to explain quantitatively the size effects in the supercooling and superheating fields of small Cd spheres on the basis of existing theories, one must assume values of ξ_0 an order of magnitude smaller than those determined for bulk samples. We have not found any explanation for this inconsistency; however, we would like to point out that it seems to be a fairly

general phenomenon. Cody and Miller, for instance, determined anomalously large values of κ for³² Pb and³³ Sn by studying size effects on the critical fields of films and foils. These values of κ —0.34 for Pb and 0.22 for Sn as opposed to 0.22 and 0.087, respectively, determined for bulk samples^{4,5}—also seem to suggest anomalously small values of ξ_0 . Measurements with films and foils of small κ materials (Al, Cd) are now in progress. They should contribute significantly to the clarification of this disagreement.

The size effect found for the critical temperature of our Cd spheres seems to be related to the removal of gap anisotropy by the presence of the boundary. If one uses the value of the anisotropy parameter recently reported³¹ and a mean free path approximately equal to the sphere radius, the theory of Markowitz and Kadanoff²⁵ also leads to a value of ξ_0 much smaller than that found for bulk samples.

Note added in manuscript. Dr. F. Rothwarf

has pointed out that a possible explanation for the quenching field in our bulk cylinder may be the presence of clusters of light isotopes of Cd, with correspondingly higher critical temperatures. His evaluation of the effect and the recent results of Fassnacht and Dillinger³⁴ indicate that this explanation is likely to be correct. It is interesting to point out that the main part of the transition at zero field takes place between 0.527 and 0.536 °K but there is still a signal different from zero to temperatures as high as 0.555 °K, where the quenching field extrapolates to zero.

ACKNOWLEDGMENTS

The authors would like to thank Professor M. Richman for his help in the electron microscopic examination of our samples and Professor G. M. Seidel for the use of his He³ refrigerator. We are also indebted to Professor A. Baratoff and Professor L. Kadanoff for helpful discussions.

*Work supported by the Advanced Research Projects Agency and the National Science Foundation.

¹F. E. Faber, Proc. Roy. Soc. (London) A241, 531 (1957).

²F. de la Cruz, M. D. Maloney, and M. Cardona, Conference on the Science of Superconductivity, Stanford University, 1969 (unpublished).

³J. Feder, J. R. Kiser, and F. Rothwarf, Phys. Rev. Letters 17, 87 (1966).

⁴J. Feder and D. S. McLachlan, Phys. Rev. 177, 763 (1969).

⁵F. W. Smith and M. Cardona, Solid State Commun. 6, 37 (1968).

⁶J. Feder, S. K. Kiser, F. Rothwarf, J. P. Burger, and C. Valette, Solid State Commun. 4, 611 (1966).

⁷F. W. Smith and M. Cardona, Phys. Letters 24A, 247 (1967).

⁸V. L. Ginzburg, Zh. Eksperim. i Teor. Fiz. 34, 113 (1958) [Sov. Phys. JETP 7, 78 (1958)].

⁹D. Saint-James and P. G. de Gennes, Phys. Letters 7, 306 (1963).

¹⁰F. W. Smith, A. Baratoff, and M. Cardona, in *Proceedings of the Eleventh International Conference on Low Temperature Physics*, edited by J. F. Allen, D. M. Finlayson, and D. M. McCall (University of St. Andrews Printing Dept., St. Andrews, Scotland, 1969).

¹¹L. P. Gorkov, Zh. Eksperim. i Teor. Fiz. 37, 1407 (1959) [Sov. Phys. JETP 10, 998 (1960)].

¹²E. Helfand and N. R. Werthamer, Phys. Rev. 147, 288 (1966).

¹³G. Eilenberger, Phys. Rev. 153, 584 (1967).

¹⁴G. Luders, Z. Physik 202, 8 (1967). This work has a numerical mistake; the correction was made by G. Luders and K. S. Usadel, Z. Physik 222, 358 (1969).

¹⁵C. R. Hu and V. Korenman, Phys. Rev. 178, 684 (1969); 185, 672 (1969).

¹⁶V. L. Ginzburg and L. D. Landau, Zh. Eksperim. i Teor. Fiz. 20, 1064 (1950).

¹⁷J. P. Burger and D. Saint-James, in *Superconductivity*,

edited by R. D. Parks (Marcel Dekker, New York, 1969), Vol. 2, p. 977.

¹⁸P. G. de Gennes, Phys. Letters, Physics 1, 107 (1964).

¹⁹W. L. Pillinger, P. S. Jastram, and J. G. Daunt, Rev. Sci. Instr. 29, 159 (1958).

²⁰E. P. Harris and D. E. Mapother, Phys. Rev. 165, 522 (1968).

²¹T. E. Faber and A. B. Pippard, in *Progress in Low Temperatures Physics*, edited by C. J. Gorter (North-Holland, Amsterdam, 1955), Vol. 1, p. 159.

²²E. A. Lynton, *Superconductivity*, 2nd ed. (Methuen, London, 1964).

²³F. W. Smith, A. Baratoff, and M. Cardona, Phys. Kondensierten Materie 12, 145 (1970).

²⁴A. Baratoff and K. Bergeron, Bull. Am. Phys. Soc. 13, 177 (1968).

²⁵D. Markowitz and Leo P. Kadanoff, Phys. Rev. 131, 563 (1963).

²⁶T. Tsuneto, Progr. Theoret. Phys. (Kyoto) 28, 857 (1962).

²⁷C. Caroli, P. G. de Gennes, and J. Matricon, J. Phys. Radium 23, 707 (1962).

²⁸W. D. Gregory, Phys. Rev. Letters 20, 53 (1968).

²⁹W. D. Gregory, P. J. Carrol, and M. A. Superata, in *Proceedings of the Twelfth International Conference on Low Temperature Physics, Kyoto, Japan, 1970* (Academic Press of Japan, Tokyo, to be published).

³⁰G. G. Greiner, K. R. Efferson, and J. M. Reynold, Phys. Rev. 143, 406 (1966).

³¹E. Ducla-Soares and J. D. N. Cheeke, in Ref. 29.

³²R. E. Miller and G. D. Cody, Phys. Rev. 173, 481 (1968).

³³R. E. Miller and G. D. Cody, Phys. Rev. 173, 494 (1968).

³⁴R. E. Fassnacht and J. R. Dillinger, Phys. Rev. B 2, 4442 (1970).